Polímeros: Ciência e Tecnologia
E-ISSN: 1678-5169
abpol@abpol.org.br
Associação Brasileira de Polímeros
Brasil

Dartora, Paula Cristina; Campomanes Santana, Ruth Marlene; Fontes Moreira, Ana Cristina

The influence of long chain branches of LLDPE on processability and physical properties
Polímeros: Ciência e Tecnologia, vol. 25, núm. 6, 2015, pp. 531-539
Associação Brasileira de Polímeros
São Carlos, Brasil

Available in: http://www.redalyc.org/articulo.oa?id=47043165002

http://dx.doi.org/10.1590/0104-1428.1732

The influence of long chain branches of LLDPE on processability and physical properties

Paula Cristina Dartora[1], Ruth Marlene Campomanes Santana[1]* and Ana Cristina Fontes Moreira[2]

[1]Department of Materials Engineering, Universidade Federal do Rio Grande do Sul – UFRGS, Porto Alegre, RS, Brazil

[2]Politecnic Institut, Universidade Estadual do Rio de Janeiro – UERJ, Nova Friburgo, RJ, Brazil

**ruth.santana@ufrgs.br*

Abstract

Two polyethylene-based on single-site metallocene catalyst (mLLDPE) were selected to characterize the effect of long chain branching (LCB) on blown film processability, optical and mechanical properties. 13C NMR and parallel plate rheology were used to identify LCB presence on LLDPEs. Blown films were produced from 100% LLDPEs using three different machine direction (MD) stretch ratios. When the same processing conditions for the two LLDPEs grades were used, better processability was observed for LLDPE with LCB. In relation to mechanical and physical properties, Elmendorf tear and optical properties were highly influenced by the presence of LCB. Tear resistance is affected by film orientation and is inversely proportional to the level of LCB in the polymer. It was observed a reduction of 50% in the MD tear strength when comparing with the polymer without LCB. However, haze decreases significantly with the presence of LCB, about 40%.

Keywords: *LLDPE, metallocene, long chain branching, NMR, rheology, mechanical properties.*

1. Introduction

Polyethylene is the most useful polyolefin in the world. It is available commercially as groups of polyethylene: high density polyethylene (HDPE), low density polyethylene (LDPE), linear low density polyethylene (LLDPE), ultra high molecular weight polyethylene (UHMWPE) and very low density polyethylene (VLDPE)[1]. Flexible packaging marketing is the major application for LLDPE. Packaging fulfills four functions: containment, protection, convenience and communication[2]. For communication one can understand that the package usually sports the name of the product and nutritional information, for example. But the package also shows the product to the costumer, so it is important that the film have low haze[2,3]. They are basically produced by blown and cast film processes. Structural parameters, such as density/crystallinity, molecular weight and its distribution, short chain branching (SCB) / long chain branching (LCB) length and amount and crystalline morphology are the key factors that control the properties.

LLDPE are produced by copolymerization between ethylene and an alfa-olefin comonomer such as 1-butene, 1-hexene or 1-octene. It results in an ethylene/alfa-olefin copolymer with many short chain branches along the polymer backbone. Ultimate developments in metallocene catalysts allowed adding LCB on LLDPE structure during copolymerization[4]. The mechanism of LCB formation is not well known, but the most accepted is a random *inter*molecular reaction although in some cases this mechanism does not explain the phenomena observed[4,5]. Another way to obtain LLDPE with long chain branches is mixing LLDPE with peroxides, using peroxide concentrations below the critical gel formation concentration[6].

There remains a need to find sensitive methods to characterize LCB architecture[7]. Gel permeation chromatography (GPC) was the first method used to detect LCB. However, it was necessary to fractionate the polymer before characterization and it was not possible to obtain quantitative information[8,9].

To quantify LCB levels, more complex analyses are needed. One widely used technique is nuclear magnetic resonance (NMR)[10]. This technique, however, has a limitation. When the alfa-olefin comonomer used to produce the polymer has more than six carbon atoms, the chemical shift observed for LCB is the same observed for the comonomer[10]. Recently, studies showed that it is possible to distinguish branches longer than six carbons, up to twenty carbon atoms, but it is necessary high resolution[11].

Nevertheless, the most sensitive method is the rheological method. Small levels of LCB, such as 1LCB / 10.000C affect the rheological behavior of the polymer[6,12]. LCB has distinct effects on different rheological quantities (zero shear-rate viscosity - η_0 - and strain hardening). This is caused by the fundamental differences between the molecular mobility of linear and long branched chains. Strain hardening and η_0 increase when LLDPE presents LCB[13]. To be able to use rheological data to compare two or more polyethylene grades, it is necessary that they have the same polydispersity[14], because long molecules in a narrow molar mass distribution can create the same rheological behavior in elongation as long-chain branches[13].

One way to detect LCB using rheological data is considering the flow activation energy of the LLDPE. LLDPE usually has a flow activation energy smaller than 28 kJ/mol. On the other hand, LDPE, which is a highly branched polymer and presents a flow activation energy

around 60 kJ/mol. When LLDPE resins have LCB, the flow activation energy increases, reaching values of about 45 kJ/mol[14].

LCB is commonly introduced into the fractions with higher molecular weight[15], decreasing the viscosity of these fractions[8]. The decreasing of viscosity improves the processability of the polymer[7,8,14]. It is especially important when metallocene-based polymers are considered, as these polymers have problems with processability caused by their narrow molecular weight distribution[14].

SCB and LCB affect polymer's density, crystallinity, resistance and processability, as they change the polymer's structure[15].

It is recognized in literature that higher levels of LCB in blown film resins improve bubble stability[7]. It is also known that LCB governs die swell, melt strength, and environmental stress crack resistance in blow molding operations, orientation in film, sag resistance in pipe and geomembranes and shear thinning and melt fracture in all extrusion processes[4].

Mechanical and physical properties are affected by polymer structure[16]. For example, haze is affected by polymer crystallinity and/or crystal structure, surface imperfections and bubbles or particles (additives) in the film[17]. Recent studies show that the LCB content in polymer chain affects the polymer crystallinity, crystal thickness, tensile strength, tensile modulus and rheological characteristics of mPELBD (m means polymer prepared via metallocene catalyst)[18]. Since LCB affects polymer crystallinity and crystal structure, it consequently affects film haze[19].

Elmendorf tear resistance is strongly dependent on film orientation. When a film is produced with an LDPE resin, increasing the film orientation increases Elmendorf tear resistance on machine direction (MD). However, when the raw material is a LLDPE, the opposite behavior is observed, decreasing significantly MD Elmendorf tear resistance when the film orientation is increased[20].

Structures of polyethylene blown films have been studied for a long time, but some concerns and controversy still exist, and some structural features and physical behaviors are not completed understood.

The aim of the present work is at evaluating the effects of LCB on the blown film properties of 1-hexene-based LLDPE resins, in order to further define and understand the processing-structure-property behavior of these resins.

2. Experimental

2.1 Materials

Two mLLDPE grades from Braskem were used in this work. Metallocene grades were produced with different types of catalysts but all of them used 1-hexene as comonomer. Table 1 shows details about the resins used.

It is important to say that the designation of the catalyst as metallocene type A or B was only used to show that the resins were produced with different catalyst systems.

Table 1. Basic resin characteristics.

Samples	mLLDPE A	mLLDPE B
Density (g/cc)	0.9176	0.9194
Melt flow index (g/10min)[a]	1.02	0.58
Catalyst	Metallocene type A	Metallocene type B
Comonomer (%wt)[b]	8	8
Mw × 10^{-3} (kg/mol)[c]	123	115
Mw/Mn[c]	1.96	3.39

[a]190°C/2.16kg. [b]Comonomer content obtained from ^{13}C NMR. [c]Mw and MWD were obtained from GPC.

2.2 Resins characterization

Samples were analyzed by ^{13}C NMR on a Varian Wibe bore 400, with a 5mm probe. Samples were prepared by dissolving 50 mg of polymer in 0.7 mL of ortodichlorobenzene and 0.2 mL of tetrachloroethane-d_2.

For long chain branching (LCB) quantification, Equation 1 was used, where α is the medium's intensity of LCB carbon atoms and T_{tot} is total carbon intensity[10].

$$Branches/10000\,carbons = \left[\frac{(1/3)\alpha/}{(T_{Tot})}\right]\times 10^4 \quad (1)$$

The samples were also analyzed by MCR501 Physica Anton Paar rheometer. Samples were prepared by compression molding, in circular shape, with 2.5 cm of diameter and 2 mm of thickness. A tension of 200 Pa was applied on a frequency sweep mode, from 0.001 to 100 Hz, at 190, 200 and 210 °C. Equation 2 was used to calculate flow activation energy for all samples[21].

$$\eta = B\times e^{\left(-E_a/(R.T)\right)} \quad (2)$$

Where: η = apparent viscosity (Pa s);

B = pre-exponential factor;

E_a = flow activation energy (J mol^{-1});

R = the universal gas constant (8.314 J mol^{-1} K^{-1});

T is absolute temperature (K).

2.3 Films production

All the blown film samples (100% LLDPE) were made on a Carnevalli CHD60 blown film line using typical linear low-density (LLDPE) conditions as follows: 200 mm die diameter; 1.8 mm die gap; 800 rpm screw speed; 2.2:1 blow up ratio (BUR); freeze line high (FLH) of about 60 cm, temperature profile from 180 to 200°C and three different film thickness: 35 μm, 60 μm and 100 μm. For output analysis, two indexes were observed using the 35 μm-thickness samples.

$$Energy\,index = amperage/output\ \left(A\ h\ kg^{-1}\right) \quad (3)$$

$$Output\,index = melt\,pressure/output\ \left(bar\ h\ kg^{-1}\right) \quad (4)$$

These indexes represent two important aspects for plastic industry: energy consumption and limit of production. Energy consumption is a cost indicator; it means that with lower

energy consumption, it is possible to reduce cost per kg of production. Output index is related to capacity of motor load; in other words, extruders have a limit of melting pressure. This parameter depends of the type of material; some of them flow easily and as a result the melting pressure is low. Other polymers are difficult to flow, increasing the melting pressure leading to stop the production.

The film samples will be identified in this paper according to Table 2.

Samples mLLDPE A_35 and mLLDPE B_35 were chosen to perform bubble stability studies, in which the only variable was the screw speed. The screw speed was increased gradually up to 75% of the machine capacity (1450 rpm) to evaluate the bubble stability of both materials. Films with 35 µm were chosen because they are the most produced by packaging industry and they have the most critical processing conditions (higher MD stretch ratio).

2.4 Film characterization

The Elmendorf tear properties of all blown films were measured according to ASTM D-1922, using a TMI Universal Tear Tester. Haze analysis follows the ASTM D1003 standard method. All samples were analyzed by a BYK-Gardner equipment. Gloss analysis at an angle of 45° was carried out following ASTM D2457 also using BYK-Gardner equipment. For the three analyses aforementioned, 10 test specimens were used. Film crystallinity was determined by DSC analysis, with a heating rate of 10 °C/min, from –20 to 200 °C. The reference value for PE 100% crystalline used was 286.6 J/g[22].

Table 2. Samples identification.

Sample	Film Thickness (µm)	MD stretch ratio
mLLDPE A_35	35	115
mLLDPE B_35	35	115
mLLDPE A_60	60	67
mLLDPE B_60	60	67
mLLDPE A_100	100	40
mLLDPE B_100	100	40

3. Results and Discussion

3.1 Resins characterization

It is possible to observe in Table 1 that the resins have the same density and amount of comonomer, but they have a different molecular weight distribution (Mw/Mn). It can be assumed that they are similar in their molecular structures in relation to SCB amount and molecular weights[23].

Initially the samples were characterized using ^{13}C NMR and rheological test. Comparative NMR spectra can be observed on Figure 1.

The chemical shifts usually observed when ethylene is polymerized using 1-hexene as comonomer are present on both spectra, according to Table 3[10]. Two characteristic LCB chemical shifts (32.32 ppm and 22.92 ppm), however, are present only for mLLDPE B. These two peaks were observed only for sample mLLDPE B and correspond to the insertion of a branch with six or more carbon atoms. As the polymer was produced using 1-hexene as comonomer, the branching formed by the comonomer insertion could not have more than four carbon atoms. The LCB level on sample mLLDPE B is about 4.7 LCB/10000C. To obtain the level of LCB, Equation 1 was used[10].

Rheological analyses of the samples were carried out at three different temperatures, as shown in Figure 2. It can be observed that the rheological behavior of both samples is different. Comparing both figures, it can be observed that the sample mLLDPE A (Figure 2a) presents the Newtonian plateau for complex viscosity when low frequencies are

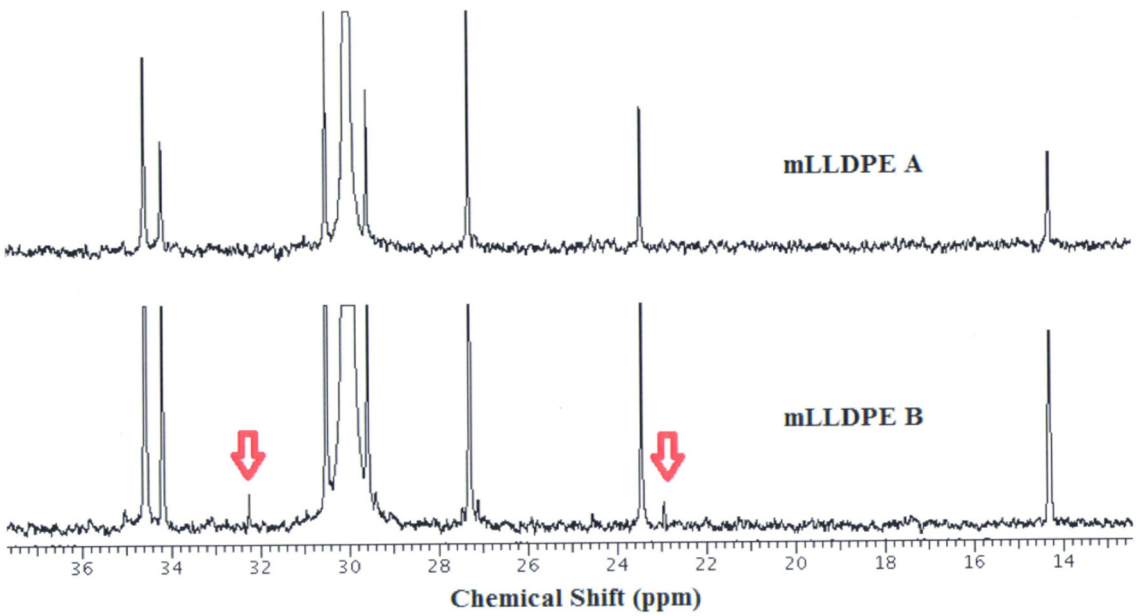

Figure 1. ^{13}C NMR spectra for LLDPE resins.

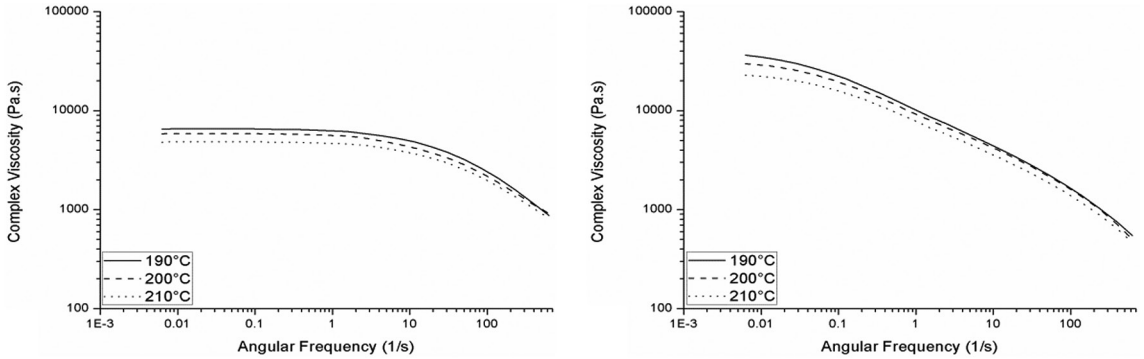

Figure 2. Rheological data obtained for the sample (a) mLLDPE A; (b) mLLDPE B.

applied (< $1s^{-1}$), while the sample mLLDPE B does not present the Newtonian plateau. These differences can be explained in accordance to earlier studies[24-27], where it is shown that the broad Newtonian plateau on the complex viscosity is characteristic of polymers that present a narrow molecular mass distribution. These are in agreement with the data shown on Table 1, where it can be seen that the mLLDPE A sample has a narrower molecular weight distribution than mLLDPE B[3,4].

It is observed that the complex viscosity of mLLDPE A is lower than the complex viscosity of mLLDPE B considering the same temperature and low frequency, although both present M_w of the same order of magnitude (Table 1). This behavior can be attributed to the larger entanglement of the mLLDPE B, caused by the presence of LCB; so, the entanglement velocity is higher than the disentanglement velocity. On the other hand, when high frequencies are applied, the situation is reversed and mLLDPE B's viscosity decreases quickly, becoming smaller than mLLDPE A's viscosity after ~500 s^{-1}[24]. LCB affects the viscosity of polymers in two ways: 1) the polymer with LCB has higher molecular weight entanglement compared to its linear polymer of the same M_w and same chemical structure; 2) the disentanglement of branched polymer is easier compared to linear polymer under shear force/stress[18].

The higher complex viscosity values observed on mLLDPE B are typical of LDPE, which are highly branched, and can indicate the presence of LCB[13]. When long branches are present in the polymer, the entanglements increase and consequently the complex viscosity increases as well as the molecular mobility is reduced[6,24].

When the rheological characterization was carried out with higher temperatures, the complex viscosity showed smaller values for both samples, as expected[24].

Table 4 shows data obtained for activation energy from Equation 2. The mLLDPE A flow activation energy is at the same level of classical short chain branched (SCB) LLDPE resins. On the other hand, the mLLDPE B flow activation energy is close to the corresponding energies of LDPE resins[14]. As ^{13}C NMR data, flow activation energy calculated from rheology data showed an indicative of LCB only for mLLDPE B[14]. Thereby, NMR and rheology analyses confirmed that only one of the samples presents LCB.

Table 3. Chemical shifts typically observed for ethylene/1-hexene copolymer with the corresponding carbon and sequence assignments.

Chemical Shift (ppm) TCE(d_2)[a]	Carbon Assignment	Sequence Assignment
38.14	Methine	EHE
34.55	$\alpha\delta^+$	EHEE+EEHE
34.17	$4B_4$	EHE
30.94	$\gamma\gamma$	HEEH
30.49	$\gamma\delta^+$	HEEE+EEEH
30.00	$\delta^+\delta^+$	$(EEE)_n$
29.56	$3B_4$	EHE
29.38	$3B_4$	EHH
27.28	$\beta\delta^+$	EHEE+EEHE
27.08	$\beta\delta$	HHEE+EEHH
23.42	$2B_4$	EHE
14.28	Methyl	EHE

[a]Deuterated Tetrachloroethane (solvent); H = Hexene; E = Ethene.

Table 4. Flow activation energy.

Samples	Flow activation energy (kJ/mol)
mLLDPE A	28
mLLDPE B	43

3.2 Films production

Bubble stability and maximum output were evaluated during blown film extrusion for samples with 35 μm-thickness films. Both samples presented dimensional stability even at high output rates, of about 1450 rpm. However, it was not possible to maintain the usual bubble shape for sample mLLDPE A when the screw speed was higher than 1200 rpm. LLDPE films are usually produced with the bubble shape observed on Figure 3a. When the screw speed became higher than 1200 rpm, it was necessary to change the bubble shape to the conformation used for LDPE films production, shown on Figure 3b.

The main goal of the blown film process is to manufacture a stable film with good physical and optical properties at a maximum production rate. In this case, the bubble shape is controlled in the area between the die exit and freeze

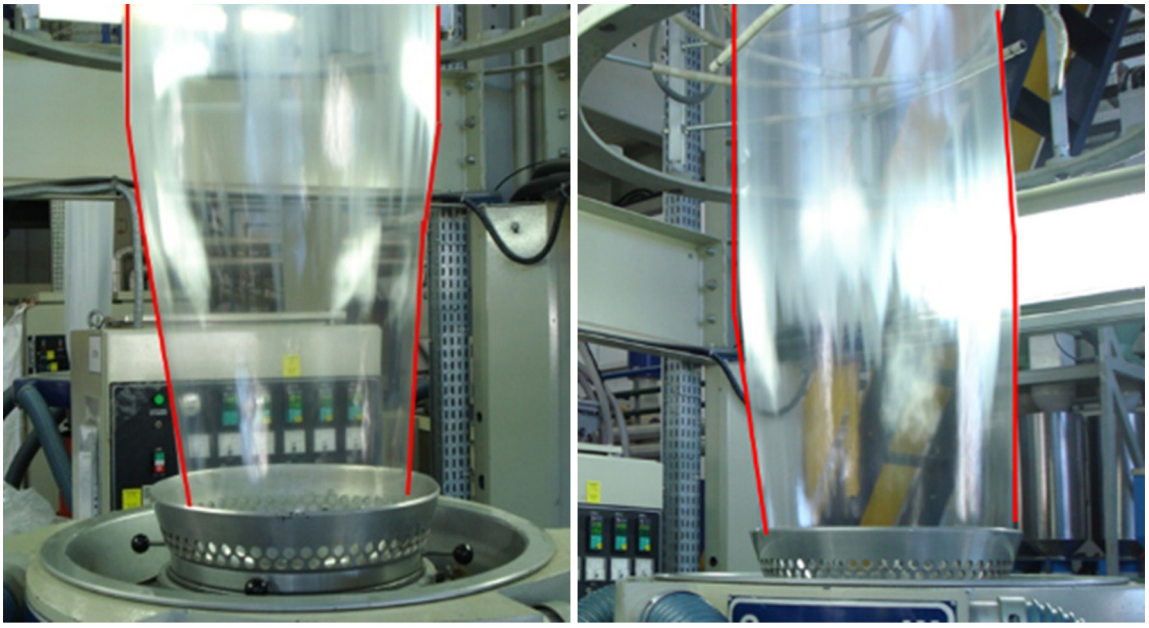

(a) (b)

Figure 3. (a) represents "LLDPE's bubble shape"; (b) represents "LDPE's bubble shape".

line height, which leads to reduced product properties, line failures, and large amounts of film scrap. Such instabilities decrease significantly the window of stable processing conditions for blown film production[28].

The maximum flow rates measured for all samples were at the same range, close to 130 kg h^{-1}. A high bubble stability, high production rate and better FLH control were obtained by mLLDPE B sample.

In relation to processability, described here as energy and output indexes, data are shown on Table 5. These indexes are inversely proportional to energy saving and output rate. Also it is observed that mLLDPE B has lower energy and output indexes, which means that mLLDPE B needs lower levels of energy (–13%) and lower melt pressure (–16%) to produce the same weight of film (1 kg) in comparison with mLLDPE A. In other words, a customer using mLLDPE B resin is able to increase their productivity with a lower energy cost, so they became more competitive.

Beyond processability characteristics, LLDPE resins have to present good optical and mechanical properties[28]. The positive effect of LCB on process parameters is already demonstrated and now, in addition, the LCB effect on optical and mechanical properties of the films will be evaluated.

Table 5. Energy and output indexes.

Samples	Energy index (A.h/kg)	Output index (bar.h/kg)
mLLDPE A	0.99	3.71
mLLDPE B	0.86	3.13
Variation B/A (%)	–13	–16

Table 6. Optical properties.

Samples	Haze (%)	Gloss 45º
mLLDPE A_35	15.2 ± 2.5	62.7 ± 5
mLLDPE B_35	10.2 ± 0.4	60.4 ± 1
mLLDPE A_60	16.7 ± 2.5	64.3 ± 4
mLLDPE B_60	9.8 ± 0.4	66.8 ± 2
mLLDPE A_100	27.1 ± 1.0	55.3 ± 4
mLLDPE B_100	11.2 ± 0.7	69.6 ± 1

3.3 Film characterization

Table 6 shows haze and gloss properties for all samples. It is possible to note that mLLDPE A exhibits higher variations on the results. The probable cause of this is the stripes formed during blown film extrusion. Figure 4 shows these stripes for mLLDPE A and no stripes for mLLDPE B during the samples manufacturing.

The stripes observed on films produced with mLLDPE A can be explained by slight differences on cooling air temperature. Film cooling is made with cold air inside and outside of the bubble. The air out of the bubble comes from small orifices, and, sometimes, temperature is not 100% homogeneous. Considering LLDPE polymers fast crystallization kinetics, these little differences are enough to produce discrepancies on film crystallization[29]. As the mLLDPE B sample possesses LCB, the crystallization kinetics is reduced, so the slight differences in cooling temperature does not disturb film homogeneity[19].

When the film thickness increases, haze values for the films produced with mLLDPE A also increase, while corresponding values for the films produced with mLLDPE B are at the same range. Gloss 45° values increase while the mLLDPE B-based films thickness increases. For the samples produced with mLLDPE A, the behavior is different. Gloss 45° values of the films with 35 µm and 60 µm are at the same range, but the film with 100 µm presents a smaller value

for Gloss 45°. Usually it is desirable to produce films with low haze and high gloss for the packaging industry when the product does not need light protection[2,30].

The lower haze observed for mLLDPE B should be explained by the absence of stripes during blown film extrusion. Other factors that could affect haze are degree of crystallization and/or crystal structure and relaxation time of polymers. It is known that LCB increases relaxation time of polymers[31,32]. Higher relaxation time allows the crystallization to occur under influence of stress elongation, causing it to form small, thin and oriented crystalline structures. Hence this film has lower haze and higher gloss[20].

The Elmendorf tear strength data are shown in Figure 5. Clearly, all samples exhibit higher values in the transversal direction (TD) when compared to the machine direction (MD). The morphological developments during blown

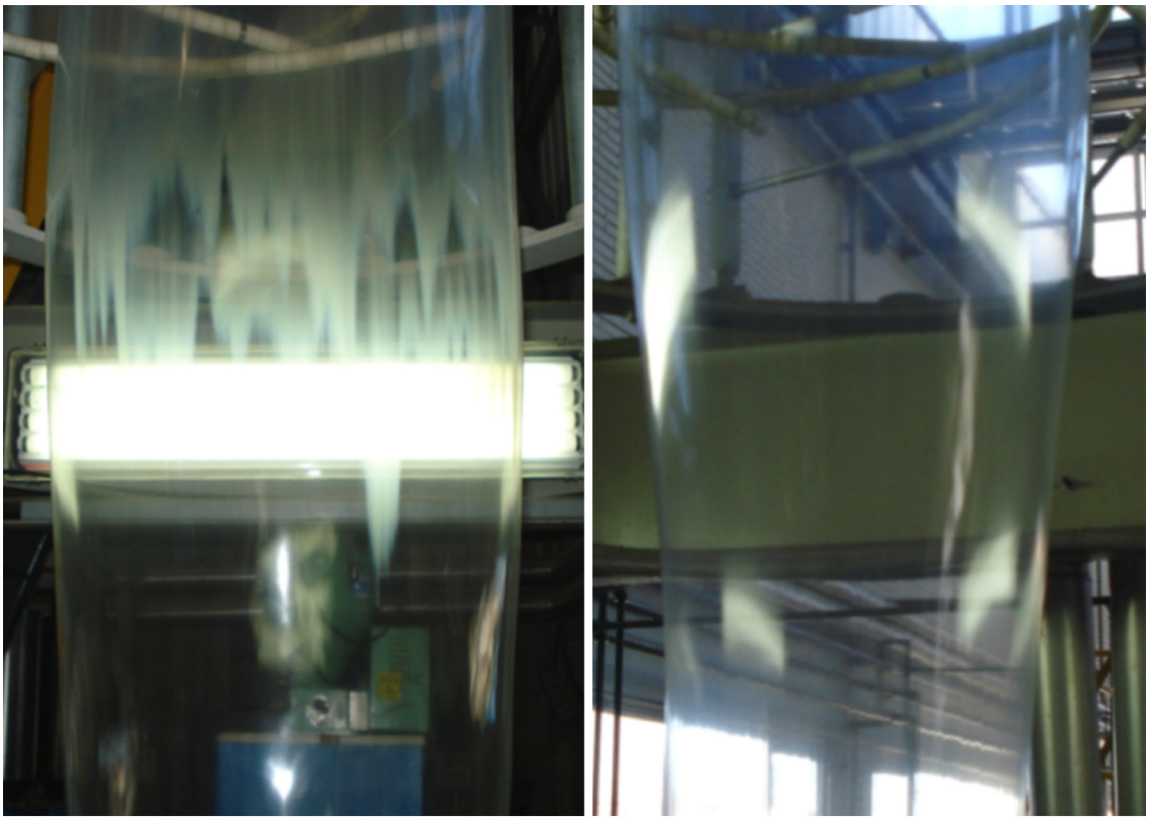

(a) (b)

Figure 4. Blown film extrusion: (a) mLLDPE A; (b) mLLDPE B.

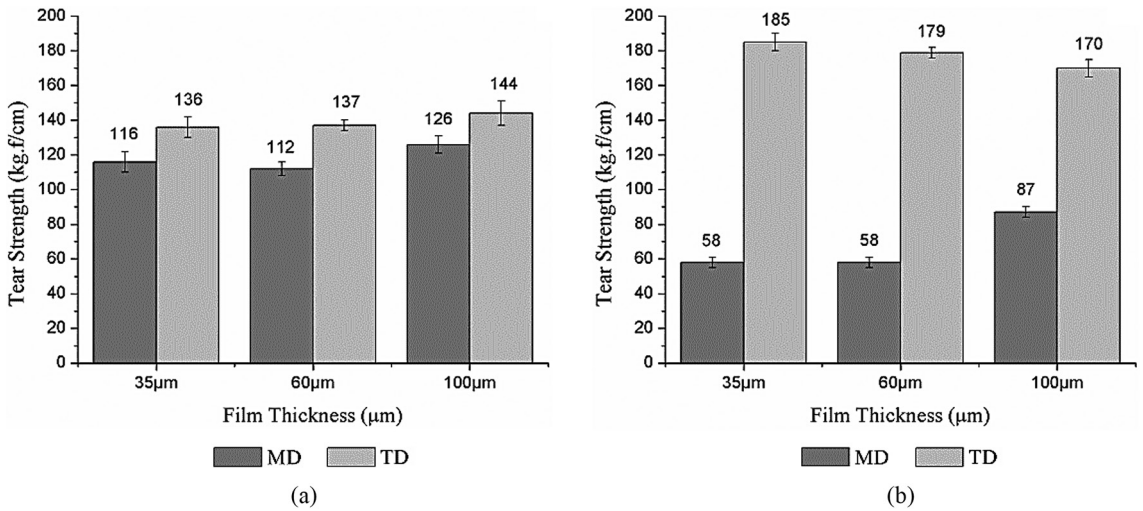

Figure 5. Elmendorf tear resistance: (a) mLLDPE A based films; (b) mLLDPE B based films.

film process for LLDPE explain the trends of tear strength TD > tear strength MD[31]. Tear strength in the MD was extremely affected by film orientation[20]. TD and MD tear strengths can be compared using the ratio of the values obtained. Table 7 shows the aforementioned ratios.

From the results above, one can deduce films produced with mLLDPE A have a better balance between MD and TD tear strength on all samples, showing a MD/TD ratio of approximately 1. On the other hand, mLLDPE B-based films have a sizeable difference between MD and TD tear strength and as a result their MD/TD ratios are smaller than 0.5 for samples with thicknesses of 35 μm and 60 μm and about 0.5 for the 100 μm-thick sample. It is known that films produced with LDPE resins have a higher tear resistance in the MD when film orientation is increased[20,31]. In the LDPE films, the twisted lamellae from adjacent row nuclei are strongly connected, which is responsible for the high MD tear. When the film orientation is increased, these connections get stronger, increasing even more the tear resistance. Films produced with LLDPE have the opposite behavior and consequently their tear strength is reduced when they are highly oriented because they usually have less oriented localized spherulite-like structures[20]. Based on this information, it can be said that the samples produced with the mLLDPE B resin present a higher level of orientation than the samples produced with mLLDPE A.

Table 7. Tear strength MD/TD ratio.

Thickness (μm)	mLLDPE A	mLLDPE B
35	0.85	0.31
60	0.82	0.32
100	0.88	0.51

When the film thickness increases, the difference between MD and TD tear strength is reduced. To increase film thickness, it is necessary to stretch it less during the manufacturing process, so the high orientation observed in the MD is reduced and, therefore, so are the differences between MD and TD tear resistances. In other words, film anisotropy is reduced.

Figure 6b clearly shows tearing in the MD for mLLDPE B_35 sample. The sample mLLDPE A 35 exhibits a rough surface on tearing propagation in the MD. The same behavior was observed for the samples with thicknesses of 60 μm and 100 μm. The observed difference in tear resistance can be associated with the crystalline lamellar structure formed at film processing. As mentioned previously, LLDPEs in general have a less oriented localized spherulite-like structure but, when long chain branches are present, it is possible that the lamellae structure get more similar to the structure observed on LDPEs, which presents twisted lamellae from strongly connected adjacent row nuclei[20].

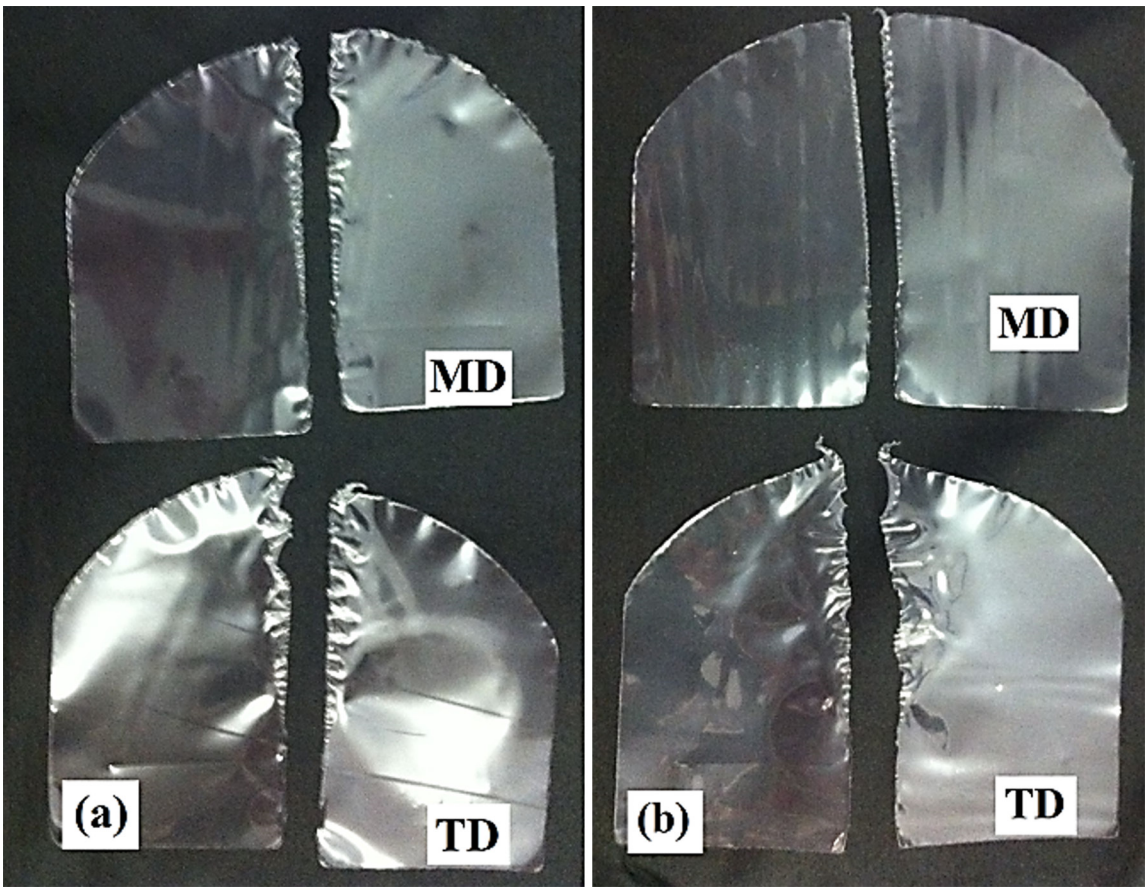

Figure 6. Elmendorf tear test specimens: (a) mLLDPE A_35; (b) mLLDPE B_35.

Table 8. Films crystallinity measured with DSC analysis.

Thickness (μm)	mLLDPE A	mLLDPE B
35	42.0	45.8
60	43.5	47.3
100	46.8	46.8

DSC results were used to calculate film crystallinity. The results are shown on Table 8.

For sample mLLDPE A, it was observed that increasing film thickness, the crystallinity also increases. On the other hand, for sample mLLDPE B, the crystallinity degree was nearly the same. Film samples with higher MD stretch ratio (35 and 60 μm) presented higher crystallinity for sample mLLDPE B, then for sample mLLDPE A. The sample with lower MD stretch ratio showed the same crystallinity degree for both samples. These results showed that crystallinity degree is not the only explanation for optical properties differences obtained. The optical differences observed for the films with different thicknesses are probably caused by crystallites shape and size, according with previously publications[22,24,31,33,34].

4. Conclusions

The presence of LCB was confirmed for one of the resins (mLLDPE B) evaluated in this study. The characterization of LCB in LLDPE was obtained by ^{13}C NMR and rheology analyses. It was clearly shown specific chemical shifts at NMR to confirm the LCB presence in mLLDPE B, and also the possibility to quantify the level of LCB/10000C. Also, rheology studies results allowed the obtention of flow activation energy for the samples and the observation of a major difference in the values of flow activation energy.

In agreement with literature, it was found that even small levels of LCB significantly altered the processability of the blown film resins. In particular, it was possible to measure the difference between resins though energy and output indexes. These data confirm that LLDPE with LCB are more prone to reduce costs during blown film extrusion.

In relation to optical properties, it was possible to confirm the positive effect of LCB on haze and gloss, independently of the film thickness, contributing for better flexible packaging films.

However, it was observed that the addition of LCB to LLDPE blown film resin resulted in a decrease in Elmendorf tear resistance. The presence of LCB is likely to produce higher levels of orientation on blown film and as a result of this a huge unbalance in tear resistance was observed. When the stretch ratio was reduced, samples presented better Elmendorf tear resistance, but a reduction in the stretch ratio results in lower productivity. The films here studied did not show significant crystallinity variations by changing film thickness. The introduction of LCB does not appear to provide an improvement for both processing and film performance, as it has been often suggested in the literature. Probably there is an optimum level of LCB that improves both processing and properties. Thence, we intend to further characterize both polymer and films samples to completely understand the LCB effect on crystallite formation during blown film process.

5. Acknowledgements

The authors would like to thank the following for their significant contributions to this work: M. A. da Silva, B. E. S. Mendonça, F. P. dos Santos, S.S. Staub and C. Ellwanger. In addition, the authors would like to thank Braskem S.A. for support and permission to publish this work and CNPq for financial support.

6. References

1. Coutinho, F. M. B., Melo, I. L., & Maria, L. C. S. (2003). Polietileno: principais tipos, propriedades e aplicações. *Polímeros: Ciência e Tecnologia*, *13*(1), 1-13. http://dx.doi.org/10.1590/S0104-14282003000100005.
2. Berk, Z. (2013) *Food packaging*. In S. L. Taylor (Ed.), *Food process engineering and technology* (pp. 621-636). London: Academic Press.
3. Kropf, D. H. (2004) *Packaging: techonology and films*. In W. K. Jensen (Ed.), *Encyclopedia of meat science* (pp. 943-949). New Zealand: Elsevier.
4. Yang, Q., Jensen, M. D., & McDaniel, M. P. (2010). Alternative View of Long Chain Branch Formation by Metallocene Catalysts. *Macromolecules*, *43*(21), 8836-8852. http://dx.doi.org/10.1021/ma101469j.
5. McDaniel, M. (2003). *Long chain branching in polyethylene from the Phillips Catalyst*. In *Proceeding of the 59th Southwest Regional Meeting of the American Chemical Society*. Oklahoma: American Chemical Society.
6. Golriz, M., Khonakdar, H. A., & Morshedian, J. (2014). Thermorheological behavior of peroxide-induced long chain branches linear low density polyethylene. *Thermochimica Acta*, *590*, 259-265. http://dx.doi.org/10.1016/j.tca.2014.07.010.
7. Munstedt, H. (2008). Rheological experiments as a versatile tool to analyse long-chain branches in polymers. *Polymer Preprints*, *49*(1), 81-82. Retrieved in 26 April 2013, from http://library.sut.ac.th:8080/ACS/V49N01Y2008/files/0192.pdf
8. Williamson, G. R., & Cervenka, A. (1974). Characterization of low-density polyethylene by gel permeation chromatography—II. Study on the Drott method using fractions. *European Polymer Journal*, *10*(3), 295-303. http://dx.doi.org/10.1016/0014-3057(74)90121-9.
9. Small, P. A. (1975). *Long-chain branching in polymers*. In *Macroconformation of polymers*. (Advances in Polymer Science, Vol. 18, pp. 1-64). Berlin: Springer-Verlag Berlin Heidelberg. http://dx.doi.org/10.1007/3-540-07252-7_1
10. Randall, J. C. (1989). A review of high resolution liquid ^{13}carbon nuclear magnetic resonance characterizations of ethylenebased polymers. *Journal of Macromolecular Science, Part C: Polymer Reviews*, *29*(2-3), 201-317. http://dx.doi.org/10.1080/07366578908055172.
11. Hou, L., Fan, G., Guo, M., Hsieh, E., & Qiao, J. (2012). An improved method for distinguishing branches longer than six carbons (B_{6+}) in polyethylene by solution ^{13}C NMR. *Polymer*, *53*(20), 4329-4332. http://dx.doi.org/10.1016/j.polymer.2012.07.053.
12. Lee, H. Y., Kim, D. H., & Son, Y. (2008). Anomalous rheological behavior of polyethylene melts in the gross melt fracture regime in the capillary extrusion: effect of long-chain branching. *Journal of Applied Polymer Science*, *107*(4), 2350-2355. http://dx.doi.org/10.1002/app.27382.
13. Stadler, F. J., Piel, C., Kaminsky, W., & Münstedt, H. (2006). Rheological characterization of long-chain branched polyethylenes and comparison with classical analytical methods.

Macromolecular Symposia, *236*(1), 209-218. http://dx.doi.org/10.1002/masy.200690057.

14. Gabriel, C., & Munstedt, H. (1999). Creep recovery behavior of metallocene linear low-density polyethylenes. *Rheologica Acta*, *38*(5), 393-403. http://dx.doi.org/10.1007/s003970050190.
15. Ramachandran, R., Beaucage, G., McFaddin, D., Merrick-Mack, J., Galiatsatos, V., & Mirabella, F. (2011). Branch length distribution in TREF fractionated polyethylene. *Polymer*, *52*(12), 2661-2666. http://dx.doi.org/10.1016/j.polymer.2011.04.005.
16. Peacok, A. J. (2000). *Handbook of polyethylene: structures, properties and applications*. New York: Marcel Dekker.
17. American Society for Testing and Materials – ASTM. (2013). *ASTM D-1003: standard test method for haze and luminous transmittance of transparent plastics*. West Conshohocken: ASTM.
18. Parvez, M. A., Rahaman, M., Soares, J. B. P., Hussein, I. A., & Suleiman, M. A. (2014). Effect of long chain branching on the properties of polyethylene synthesized via metallocene catalysis. *Polymer Science, Series B*, *56*(6), 707-720. http://dx.doi.org/10.1134/S156009041466004X.
19. Butler, T. I. (2009). *PE Processes*. In J. R. Wagner Jr. (Ed.), *Multilayer flexible packaging* (pp. 15-30). Oxford: William Andrew.
20. Borse, N., Aubee, N., & Tas, P. (2010). *Enhancement in tear properties of single-site catalyzed LLDPE blown films at higher draw-down*. In *Proceedings of the 26th Polymer Processing Society Annual Meeting*. Banff-Canadá: Polymer Processing Society.
21. Rigo, M., Bezerra, J. R. M. V., & Córdova, K. R. V. (2010). Estudo do efeito da temperatura nas propriedades reológicas da polpa de butiá (Butia eriospatha). *Ambiência - Revista do Setor de Ciências Agrárias e Ambientais*, *6*(1), 25-36. Retrieved in 05 May 2013, from http://revistas.unicentro.br/index.php/ambiencia/article/view/972/973
22. Becker, M. R., Forte, M. M. C., & Baumhardt, R., No (2002). Preparação e avaliação térmica e reológica de mistura de PEBD/PELBD. *Polímeros: Ciência e Tecnologia*, *12*(2), 85-95. http://dx.doi.org/10.1590/S0104-14282002000200007
23. Kulin, L. I., Meijerink, N. L., & Starck, P. (1988). Long and short chain branching frequency in Low Density Polyethylene (LDPE). *Pure and Applied Chemistry*, *60*(9), 1403-1415. http://dx.doi.org/10.1351/pac198860091403.
24. Bueche, F. (1962). *The physical properties of polymers*. New York: John Wiley&Sons.
25. Bretas, R. E. S. & D'avila, M. A. (2000). *Reologia de polímeros fundidos*. São Carlos: UFSCar.
26. Dealy, J. M., & Wissbrun, K. F. (1990). *Melt rheology and its role in plastics processing*. London: Chapman&Hall.
27. Malkin, A. Y. (1994). *Rheolgy fundamentals*. Toronto: ChemTec.
28. Butler, T. I. (2005). *Film extrusion manual: process, materials, properties*. Norcross: Tappi Press.
29. Guerrini, L. M., Paulin, F. P. I., & Bretas, R. E. S. (2004). Correlação entre as propriedades reológicas, óticas e a morfologia de filmes soprados de LLDPE/LDPE. *Polímeros: Ciência e Tecnologia*, *14*(1), 38-45. http://dx.doi.org/10.1590/S0104-14282004000100012
30. Alvarez, V. B., & Pascall, M. A. (2011). *Packaging*. In J. W. Fuquay (Ed.), *Encyclopedia of dairy sciences* (pp. 16-23). New York: Academic Press.
31. Zhang, X. M., Elkoun, S., Ajji, A., & Huneault, M. A. (2004). Oriented structure and anisotropy properties of polymer blown films: HDPE, LLDPE and LDPE. *Polymer*, *45*(1), 217-229. http://dx.doi.org/10.1016/j.polymer.2003.10.057.
32. Krishnaswamy, R. K., & Sukhadia, A. M. (2000). Orientation characteristics of LLDPE blown films and their implications on Elmendorf tear performance. *Polymer*, *41*(26), 9205-9217. http://dx.doi.org/10.1016/S0032-3861(00)00136-1.
33. Dartora, P. C., Moreira, A. C. F., Stocker, M. K., & Santos, F. P. (2013). *Análise de polietileno linear de baixa densidade metalocênico por microscopia: efeito de ramificações longas*. In *Anais do 12° Congresso Brasileiro de Polímeros*. Florianópolis: Associação Brasileira de Polímeros.
34. Liu, Z. J., Ouyang, J., Zhou, W., & Wang, X. D. (2015). Numerical simulation of the polymer crystallization during cooling stage by using level set method. *Computational Materials Science*, *97*, 245-253. http://dx.doi.org/10.1016/j.commatsci.2014.10.038.

Received: Mar. 27, 2014
Revised: Mar. 26, 2015
Accepted: June 23, 2015